Sensitive Multicolor Visual Detection of Telomerase Activity Based on Catalytic Hairpin Assembly and Etching of Au nanorods

Danni Wang, Rui Guo, Yunyun Wei, Yingzhi Zhang, Xiayu Zhao, Zhangrun Xu

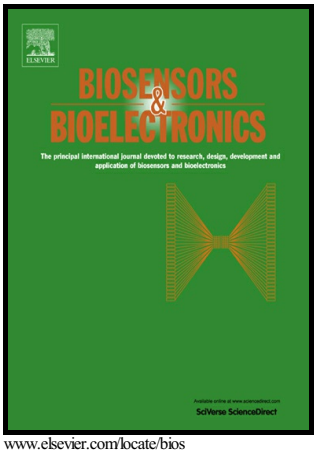

www.elsevier.com/locate/bios

PII: S0956-5663(18)30761-9
DOI: https://doi.org/10.1016/j.bios.2018.09.064
Reference: BIOS10804

To appear in: *Biosensors and Bioelectronic*

Received date: 1 August 2018
Revised date: 14 September 2018
Accepted date: 18 September 2018

Cite this article as: Danni Wang, Rui Guo, Yunyun Wei, Yingzhi Zhang, Xiayu Zhao and Zhangrun Xu, Sensitive Multicolor Visual Detection of Telomerase Activity Based on Catalytic Hairpin Assembly and Etching of Au nanorods, *Biosensors and Bioelectronic,* https://doi.org/10.1016/j.bios.2018.09.064

Sensitive Multicolor Visual Detection of Telomerase Activity Based on Catalytic Hairpin Assembly and Etching of Au nanorods

Danni Wang, Rui Guo, Yunyun Wei, Yingzhi Zhang, Xiayu Zhao, Zhangrun Xu*

Research Center for Analytical Sciences, Northeastern University, Shenyang, 110819, P. R. China.

xuzr@mail.neu.edu.cn

Abstract

Detection of telomerase activity is crucial for the telomerase-related early diagnosis of cancer and drug screening. Herein, a multicolor visual telomerase detection method with high sensitivity was developed based on the etching of hexadecyl trimethyl ammonium bromide -stablized Au nanorods (Au NRs) by the oxidation state 3,3′,5,5′-tetramethylbenzidine sulfate (TMB^{2+}). In order to meet the demand of bare-eye inspection, an enzyme-free signal amplification strategy of catalytic hairpin assembly (CHA) was incorporated. After the introduction of telomerase, telomerase extension products specifically triggered cyclic CHA and led to the successive formation of G-quadruplex/hemin DNAzyme, which catalyzed the H_2O_2-mediated oxidation of TMB. The Au NRs were gradually etched as the concentration of catalysate TMB^{2+} increased, resulting in the decrease of aspect ratio of the Au NRs. Correspondingly, the longitudinal localized surface plasmon resonance peak of Au NRs was blue-shifted, with the concomitant generation of a series of color transition. Under optimal conditions, a highly sensitive detection toward telomerase was realized down to 15 HeLa cells. Compared to previous colorimetric method for telomerase determination, multiple colors corresponding to telomerase activity was the most attractive virtue of our approach. More strikingly, telomerase-induced cyclic CHA significantly enhanced the accumulation of G-quadruplex/hemin DNAzyme, thus the signal amplification was effectively realized. Our approach exhibited excellent sensitivity and convenient signal readout, which is expected to provide great potential application in cancer diagnosis and therapy.

Keywords: Telomerase, Multicolor visual detection, Plasmonic biosensor, Catalytic hairpin assembly, Au nanorods

1. Introduction

Telomerase, a ribonucleoprotein complex, catalyzes the addition of repeat units $(TTAGGG)_n$ to the 3' end of telomere to protect the chromosome ends against fusion (Blackburn, 1991). In normal somatic cells, telomerase activity is inhibited and telomere length progressively shortens during each cycle of cell division. In contrast, in more than 85% tumor cells, telomerase is highly reactivated and allows immortal cell proliferation (Shay and Bacchetti, 1997; Shay and Wright, 2005). Therefore, telomerase has been widely recognized as a remarkable biomarker and a potential therapeutic target for cancer treatment.

In recent decades, numerous telomerase detection strategies were developed. Among them,

polymerase chain reaction (PCR)-based telomeric repeat amplification protocol (TRAP) is a gold-standard method (Kim et al., 1994), which displays extraordinary sensitivity, but is limited by time-consuming procedure and sophisticated manipulation. In addition, false negative signals may be generated due to the presence of some polymerase inhibitors in clinical samples (Yaku et al., 2017). To overcome above-mentioned deficiencies, multifarious alternative PCR-free approaches have emerged for the detection of telomerase activity, including fluorescence (Fu et al., 2018; Gao et al., 2016), electrochemistry (Liu et al., 2017a; Liu et al., 2017b), colorimetry (Duan et al., 2014; Freeman et al., 2010; Li et al., 2015; Zhang et al., 2016), chemiluminescence (Wang et al., 2013), surface enhanced Raman scattering (SERS) (Ma et al., 2017a; Shi et al., 2016), and so on. Compared to other methods, colorimetry is a prevailing strategy owing to its unique advantages such as simplicity, inexpensiveness, ease-of-use and accessibility. Especially, colorimetric analysis is suited for point-of-care detection because the results are able to be read out by naked eyes. Owing to the above merits, numerous colorimetric methods have been developed for telomerase activity determination. These methods are predominantly classified into two categories in terms of their detection principles. One is gold nanoparticles (Au NPs) aggregation-based biosensing, which relies on the fact that elongated primers of telomerase induce the formation of cross-linking assembly or the aggregation of Au NPs, resulting in a strong plasmon coupling between the nearby particles and causing an obvious color transition from red to blue (Duan et al., 2014; Zhang et al., 2016). Nevertheless, prelabeling of DNA probes on Au NPs is costly and cumbersome. Furthermore, the aggregation extent of Au NPs is influenced by many factors, which results in non-specific interference. Especially for complicated samples, self-aggregation of Au NPs occurs and inevitably leads to a false signal. Another kind of universal method is based on the notable horseradish peroxidase (HRP)-mimicking catalytic activity of telomeric G-quadruplexes/hemin DNAzyme, which effectively catalyzes the H_2O_2 mediated oxidation of 3,3′,5,5′-tetramethylbenzidine sulfate (TMB) or 2,20-azinobis (3-ethylbenzothiozoline)-6-sulfonic acid (ABTS), accompanied by a color change (Freeman et al., 2010; Li et al., 2015). Such type of method is not quite satisfactory to fulfill the sensitive detection of telomerase by naked eyes, for it only presents monochromic intensity change. Furthermore, mimic enzymes own relatively low catalytic efficiency, and telomeric G-quadruplexes have the potential to inhibit the telomerase activity. For these limitations, it is necessary to develop a facile and reliable colorimetric method with high sensitivity for telomerase activity detection.

Notably, compared to optical density change, the color variation with spectral peak shift is more easily discriminated by naked eyes. Since the surface plasmon resonance peaks of noble metal nanostructures are highly dependent on their size, shape and composition, plenty of colors are presented when growth or etch occurs (Truong et al., 2014). Lin's group utilized a new oxidation reagent TMB^{2+} for quantitative etching of Au nanorods, integrating with commercially available HRP-TMB immunoassay kit, and the typical biomarkers of carcinoma embryonic antigen (CEA) and prostate specific antigen (PSA) were analyzed with naked eyes (Ma et al., 2017b). As an essential peroxidase substrate, TMB has been widely applied for developing the colorimetric assay (Kong et al. 2018; Liao et al. 2017; Singh et al. 2017). Among mimic peroxidases, the G-quadruplexes/hemin DNAzyme could be a promising candidate to catalyze the generation of TMB^{2+} for subsequent etching of Au NRs, because it owns stability and cost-effective advantages, though only affording catalytic efficiency inferior to that of protein enzyme HRP (Yang et al., 2017). This disadvantage seriously confines the sensitivity of

DNAzyme-catalyzed assay. To circumvent this limitation, signal amplification strategies is expected to provide a feasible way. Catalytic hairpin assembly (CHA) is an isothermal, enzyme-free process to generate hybridized duplexes through target-mediated self-assembly of a pair of metastable hairpin DNAs (Lee et al., 2017). The hybridization between two hairpins consequently recycles the target for the next circle, resulting in signal amplification. Owing to the virtues of being isothermal and enzyme-free, CHA has been explored extensively for sensitive detection of various targets (Cheng et al., 2018; Dai et al., 2017; Xu et al., 2015).

Herein, telomerase-initiated CHA process was integrated with AuNRs etching reaction to develop a facile and sensitive approach for visual telomerase detection. To facilitate the improvement of sensitivity, an enzyme-free signal amplification strategy, CHA, was introduced to increase the amount of HRP-mimicking DNAzyme, which served as catalyst to control the concentration of TMB^{2+}. Our method involves three core sections: 1) telomerase extension products triggered CHA to accumulate a massive of G-quadruplexes/hemin DNAzyme; 2) the HRP-mimicking DNAzyme catalyzed oxidation between H_2O_2 and TMB; 3) the catalysate TMB^{2+} induced gradually etching of Au NRs. Consequently, spectral evolution of Au NRs gave rise to vivid color changes of the colloidal solutions, which reflected the telomerase activity. Thanks to the G-quadruplexes/hemin DNAzyme produced in situ on the basis of telomerase-triggered formation, the labeling process of enzyme was avoided and the assay was simplified. Moreover, CHA further amplified the signal to motivate the visual detection with naked eyes. Considering the capacity of Au NRs with different aspect ratios to display plenty of vivid colors, the efficient and easy signal output can be expected. On the basis of these advantages, the sensitive visual method will be an excellent protocol toward telomerase activity detection, and a promising strategy for cancer diagnosis and drug screening.

2. Materials and methods

2.1 Materials

Hexadecyl trimethyl ammonium bromide (CTAB, ≥99.0%), ethylene glycol-bis (β-aminoethyl ether) N,N,N',N'-tetraacetic acid (EGTA) and hemin were purchased from Macklin Biochemical Co., Ltd. (Shanghai, China). Chloroauric acid ($HAuCl_4 \cdot 4H_2O$), sodium borohydride ($NaBH_4$) and ascorbic acid were purchased from Sinopharm Chemical Reagent Co., Ltd. (Shanghai, China). Silver nitrate ($AgNO_3$) was obtained from Sigma-Aldrich (St. Louis, Mo, USA). 5-bromosalicylic acid (5-BrSH) was purchased from Aladdin Chemical Reagent Co., Ltd. (Shanghai, China). Dulbecco's modified Eagle's medium (DMEM), fetal bovine serum (FBS), penicillin, streptomycin and trypsin were acquired from Hyclone Thermofisher (Beijing, China). The 1×CHAPS lysis buffer was purchased from Millipore (Bedford, MA, USA). The deoxynucleotide triphosphate (dNTP) mixture and recombinant RNase inhibitor were purchased from TaKaRa Bio Inc. (Dalian, China). Diethyl pyrocarbonate (DEPC)-treated deionized water was obtained from Sangon Biotechnology Co., Ltd. (Shanghai, China). TMB bi-component substrate was purchased from Solarbio Co., Ltd. (Beijing, China). 4S red plus nucleic acid gel stain was purchased from BBI Life Sciences (Markham, Ontario, Canada). Unless otherwise specified, all reagents were used as received without further purification. Deionized water was used throughout the experiments.

Hemin stock solution was prepared in DMSO and stored in the dark at -20°C. The oligonucleotides used in this work were synthesized by Sangon Biotechnology Co., Ltd.

(Shanghai, China) and their sequences were listed in Table S1.

2.2 Synthesis of Au NRs

Au NRs were synthesized according to a seed-mediated growth method. In order to obtain Au NRs with higher aspect ratio, organic additive 5-bromosalicylic acid (5-BrSA) was introduced (Ye et al., 2012). 5-BrSH has been employed to inhibit growth on the lateral faces of the Au NRs, giving rise to a preferential reduction on the tips (Scarabelli et al., 2013). A 20-mL glass vial and a stir bar were first cleaned with aqua regia for 15 min before use. An aqueous solution of gold seeds was prepared by first mixing 5 mL of 0.5 mM $HAuCl_4 \cdot 4H_2O$ with 5 mL of 0.2 M CTAB. 0.6 mL of 0.01 M freshly prepared ice-cold $NaBH_4$ was injected into the mixture with vigorous stirring. The solution color changed from yellow to brownish-yellow, and the stirring was stopped after 2 min. The seed solution was aged at 30°C for 1 h before use. For the synthesis of the growth solution, 0.91 g of CTAB together with 0.11 g 5-BrSH were dissolved in 25 mL of warm water (60°C) in a 100 mL conical flask. After this mixed solution cooled to room temperature, 1.8 mL of 4 mM $AgNO_3$ was added to it. The mixture was kept undisturbed at 30°C for 15 min, after which 25 mL of 1 mM $HAuCl_4$ solution was added. After 15 min of slow stirring (400 rpm), 190 μL of 64 mM ascorbic acid was added, and the solution was vigorously stirred for 30 s until it became colorless. The Au NRs were finally obtained after 80 μL of the seed solution was injected into the growth solution and left undisturbed at 30°C for 12 h. The as-synthesized Au NRs were purified by centrifugation at 10000 rpm for 10 min, and washed with water for three times. The precipitate was collected and redispersed in 0.05% CTAB for further use. The size and morphology of the Au NRs were observed under a transmission electron microscopy with an accelerating voltage of 200 kV (TEM, FEI Tecnai G2 F20, USA).

2.3 Cell culture and telomerase extraction

HeLa (Human cervical cancer) cells were cultured in DMEM supplemented with 10% (v/v) heat-inactivated FBS and 1% (v/v) penicillin-streptomycin solution at 37°C in a humidified atmosphere containing 5% CO_2.

For telomerase extraction, cells were collected in the exponential phase of growth, and 1×10^6 cells were dispersed in a 1.5-mL EP tube, washed twice with ice-cold PBS (0.1 M, pH 7.4), and resuspended in 200 μL of ice-cold 1×CHAPS lysis buffer. The cell mixture was incubated for 30 min on ice and centrifuged at 14000 rpm at 4°C for 20 min. The supernatant was carefully collected and transferred to a fresh 1.5-mL EP tube. The extracts were used immediately or frozen at -80°C for further use. All the tubes and tips were RNase-free.

2.4 Telomerase extension

Telomerase extracted from a certain number of cells was serially diluted in 1×CHAPS lysis buffer, and then 2 μL telomerase extracts were incubated with telomerase extension reaction buffer (20 mM Tris-HCl, pH 8.3, 1.5 mM $MgCl_2$, 63 mM KCl, 0.05% Tween 20, 1 mM EGTA, 1 mM dNTPs, 0.2 μM telomerase primer and 0.4 $U\cdot\mu L^{-1}$ recombinant RNase inhibitor). The solution was incubated at 37°C for 1 h. Then the solution was heated at 95°C for 10 min to end the extension reaction. The entire reaction was conducted under protection from light. For the negative control experiment, CHAPS lysis buffer was used to replace telomerase extracts. For thermal inactivation control experiment, telomerase extracts were heat-treated to 95°C for 10 min

before use.

2.5 Telomerase activity detection

Before the experiment, hairpin DNA 1 (H1) and hairpin DNA 2 (H2) were separately heated to 95°C for 5 min, followed by gradually annealing to room temperature with a speed of 1°C/min by a PCR machine to form hairpin structures, and stored at 4°C for further use. Subsequently, the telomerase extension products (incubated with a series of different number of HeLa cells) were added to the buffer (50 mM Tris-HCl, pH 7.5, 5 mM $MgCl_2$) containing 300 nM H1 and 300 nM H2. The mixtures were incubated at 37°C for 40 min. After that, 5 mM KCl and 1 μM hemin were respectively added to the preceding reaction solution. The solution was stood for 30 min at room temperature to form the G-quadruplexes/hemin DNAzyme. The solution system then was incubated with 50 μL TMB/H_2O_2 substrate to conduct HRP-mimicking reaction at room temperature. 30 min later, the process was terminated by introducing equal volume 1 M HCl. Finally, 100 μL Au NRs were introduced to the solution with sufficient oscillation. After 2 min, the color of the system was recorded by a digital camera. In addition, UV-vis absorption spectra of Au NRs solutions were measured under room temperature using a microplate spectrophotometer (BioTek, Synergy H1, USA). The absorption spectra of the solution were collected from 400 to 900 nm with a step of 1 nm.

2.6 Polyacrylamide gel electrophoresis (PAGE) analysis

Different DNA solutions mixed with 6×loading buffer were separately loaded onto a 12.5% native polyacrylamide gel in 1×Tris-borate-EDTA (TBE) buffer. Electrophoresis was performed on a DYCP-31 BN electrophoresis analyzer (Liuyi Instrument Company, China) under a constant voltage of 200 V for 1 h, and the gels were stained with 4S Red Plus for about 40 min. Products in the gel were visualized and photographed with ultraviolet illumination gel imaging analysis system (Life Science Research Products and System Engineering, China). The gel was prepared by using 4 mL of polyacrylamide (30%), 5 μL of TEMED, 1 mL of 10×TBE, and 50 μL of ammonium persulfate (10%).

2.7 Conventional TRAP assays

TRAP assay was performed according to the previous report (Kim et al., 1994). In brief, telomerase extracts accounting to 500 cells were used to accomplish telomerase extension reaction. Then, 5 μL of telomerization products were added into 45 μL of reaction solution containing telomerase substrate (TS) primer (0.4 μM), anchor reverse primer (ACX, 0.4 μM), dNTPs (0.2 mM), Taq DNA polymerase (2.5 U). Then, PCR was carried out using a My Cycler thermal cycler (Bio-Rad, USA) with the following program: 94°C for 4 min; 30 cycles at 94°C for 30 s, 59°C for 30 s, and 72°C for 30 s; 72°C for 5 min; 4°C hold. After PCR, the products were analyzed by PAGE.

3. Results and discussion

3.1 Principle of the proposed method

The principle for the visual detection of telomerase based on CHA and etching of Au NRs is illustrated in Scheme 1. In this biosensing system, a pair of metastable hairpin DNA probes was applied to carry out CHA. Initially, the G-quadruplex forming sequences were locked in the stem

of H2. In the absence of telomerase, the TS primers couldn't be elongated and the G-quadruplex forming sequences remained in the stem-loop structures stably, which impeded the generation of HRP-mimicking DNAzyme for subsequent etching reaction. Conversely, under the action of active telomerase, the TS primers were elongated (step 1), and the hybridization reaction between the elongated products and H1 took place via toehold-mediated strand displacement, triggering the unfolding of H1 (step 2). Subsequently, the freshly exposed sticky end of H1 hybridized to H2 and consequently the elongated products were dissociated for participating in the next cycle, resulting in dramatic accumulation of duplex DNA assemblies with active G-quadruplex-forming sequences at their end (step 3). After binding to hemin, the G-quadruplex-forming sequences folded into G-quadruplex/hemin DNAzyme (step 4), which exhibited HRP-mimicking activity. The DNAzyme catalyzed the oxidation reaction between TMB and H_2O_2 to generate TMB^{2+} in acidic solution (step 5), enabling TMB^{2+} to etch Au NRs and decrease their aspect ratio (step 6). Correspondingly, the longitudinal localized surface plasmon resonance (LSPR) peak of Au NRs was shifted, accompanied by a series of color transition. In view of the proposed facile scheme, telomerase activity can be detected by naked eyes based on solution color variations or accurately quantitated via the microplate spectrophotometry in terms of the corresponding LSPR band shifts of Au NRs. Notably, once the telomerase initiated extension, the CHA among two hairpin DNA could be performed circularly, which further increased the amount of TMB^{2+} for enhancing etching reaction. Given the exponential amplification of CHA, our approach will be expected to exhibit high sensitivity.

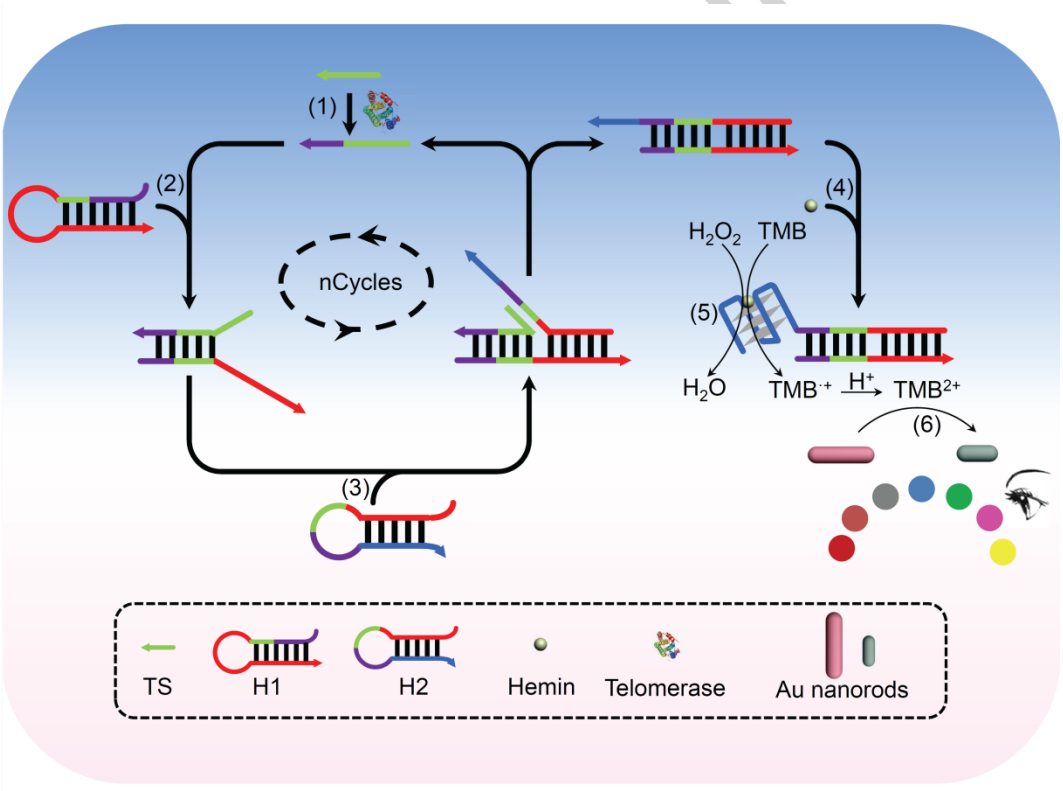

Scheme 1 Schematic illustration of the principle for multicolor visual detection of telomerase based on catalytic hairpin assembly and etching of Au nanorods.

3.2 Feasibility of the multicolor biosensing

To evaluate the feasibility of the sensing mechanism, the effect of the TMB^{2+} on the etching

of Au NRs was first investigated. The anisotropic Au NRs possess two LSPR peaks, and the longitudinal LSPR wavelength is tightly dependent on the aspect ratio. Thus, the AuNRs were selected as etching substrate. The TMB^{2+} alone just presented various intensities of yellow (Fig. 1A), which could be quantitated by measuring the absorbance at 452 nm (Fig. 1B) but was difficult for discrimination by human eyes. Upon the addition of Au NRs, the solution color changed vividly from red to gray, pale, cyan, blue, violet, purple, pink, colorless and yellow. The Fig. 1C shows that the longitudinal LSPR band of Au NRs gradually blue shifted and decreased in intensity as the concentration of TMB^{2+} increased, while the transverse LSPR band remained constant at 520 nm and only decreased in intensity. Integrating the variation of UV-vis spectra and the colors of colloid solutions, we infer that the process of etching reaction includes four stages. Firstly, the solution color changed from red to gray, pale, cyan, blue, violet and purple, and the longitudinal LSPR band gradually blue shifted. This is because the etching reaction preferentially occurred on the tips, giving rise to a decreased aspect ratio of Au NRs. Subsequently, the solution color became pink, and the longitudinal LSPR band disappeared, suggesting the transformation of nanorods into nanospheres. In addition, the colorless solution manifested that the nanospheres had been dissolved completely. Finally, the excessive TMB^{2+} render the solution a yellow color, as revealed by the disappearance of extinction peak at 520 nm and the emergence of a new band at 450 nm. In the first stage, the longitudinal LSPR shift of Au NRs ($\Delta\lambda$) displayed a good linear correlation with concentration of TMB^{2+} (see Fig. S1**)**. These phenomena clearly indicate the TMB^{2+} is capable of quantitatively etching Au NRs.

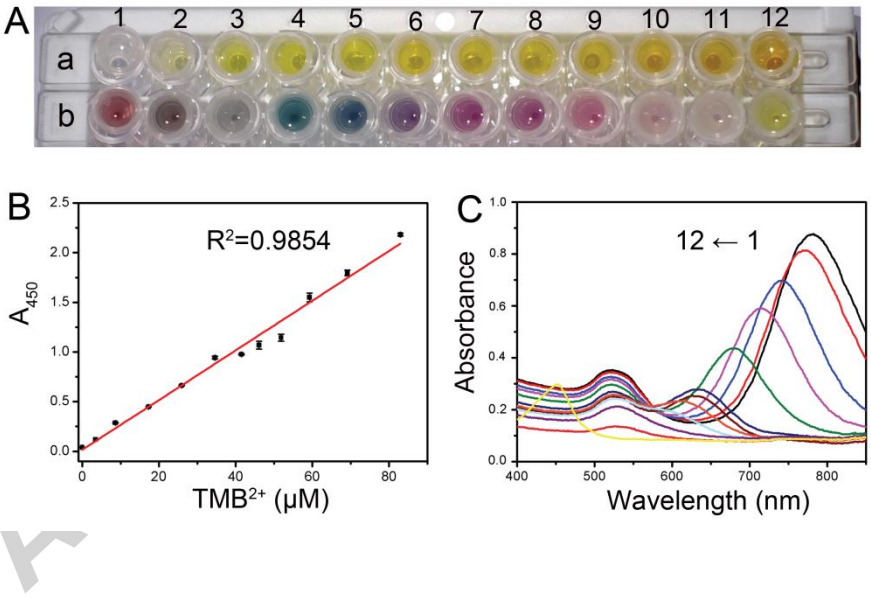

Fig. 1 (A) Photographs of the different concentrations of TMB^{2+} before (a) and after (b) the addition of Au NR solution. (B) The relationship between the absorbance at 452 nm and the concentration of TMB^{2+} before the addition of Au NR solution. (C) After the addition of the Au NR solution, the UV-vis absorption spectra of Au NR etched by different concentrations of TMB^{2+}. From 1 to 12, concentrations of TMB^{2+} were 0, 3.46, 8.64, 17.3, 25.9, 34.6, 41.5, 46.1, 51.7, 59.3, 69.2 and 83.0 μM, respectively.

On the other hand, it is essential to confirm that the CHA strategy is specifically initiated by the telomerase extension products with telomeric repeated sequence. To this end, synthetic nucleic acid was employed as a model of telomerase extended product (TEP) to validate CHA process by means of PAGE analysis. From Fig. 2A, clear bands were observed for H1 and H2, respectively

(lane 1 and 2). The mixture of H1 and H2 did not yield a new band, indicating the two DNAs were co-existing stably because of the kinetically locked (lane 3). After incubation of the TS primer with H1 and H2, bands were observed at the same positions as H1 and H2 (lane 4), which means no hybridization occurred among the TS, H1 and H2. Thus, the TS primer had little effect on the background signal. Upon addition of the TEP to the mixture of H1 and H2, an obvious band with much lower migration above H1 and H2 was displayed, while the intensity of bands ascribing to H1 and H2 decreased. This suggests that the CHA was successfully triggered by TEP, resulting in a high yield of thermodynamically favorable configuration, H1-H2 duplexs.

In support of above investigations, we then integrated plasmonic biosensing with CHA signal amplification strategy for visual monitoring of telomerase activity. To verify the capability of the proposed approach to detect telomerase activity, extracts from telomerase-positive HeLa cells were utilized as a model, and the longitudinal LSPR peak of Au NRs under different conditions were explored in detail. As depicted in Fig. 2B, the as-synthesized Au NR solution was red and exhibited a typical longitudinal LSPR band at 758 nm (curve a). Without the CHA process, the system, which only included telomerase extended product, exhibited inappreciable shift on the extinction spectrum of Au NRs, and the solution was still red (curve b vs. a). The extended product of TS primers by telomerase could fold into G-quadruplex/hemin complex structures with the help of K^+, which stands a chance to induce etching of Au NRs, nevertheless, the amount of the telomeric G-quadruplex/hemin complexes was little and their catalytic efficiency was relatively low. However, compared to the initial Au NRs (curve c vs. a), the incubation of H1 and H2 induced slight blue-shift of LSPR band, which was attributed to the weak non-specific self-assembly between H1 and H2 (Li et al., 2016) and can be denoted as low background signal. When the TS primers were elongated by telomerase in the lysate of 1000 HeLa cells, followed by incubation with H1 and H2, remarkable shift of longitudinal LSPR of Au NRs from 758 to 669 nm was observed (curve d), with the obvious color transition from red to gray. Such apparent signal variation arises from the fact that telomerase elongated products triggered the CHA and abundant G-quadruplex forming sequences were exposed for subsequent generation of HRP-mimicking DNAzyme. These DNAzymes catalyzed the conversion of TMB to TMB^{2+} under acidic condition, which could etch Au NRs quickly, giving rise to the decrease in their aspect ratio. For the heat-inactivated telomerase, the extinction spectrum (curve e) is similar to curve b, since the inactive telomerase was unable to elongate the TS primer for launching the CHA, and strikingly, the background signal originated from self-assembly between H1 and H2 was inhibited by the cell lysate. The aforementioned phenomenon demonstrates that the longitudinal LSPR shift of Au NRs is strongly related to the telomerase activity. Moreover, vivid color variation was easily observed from the inset in Fig. 2B by naked eyes. Therefore, the proposed method is entirely feasible for telomerase activity determination in cell extract.

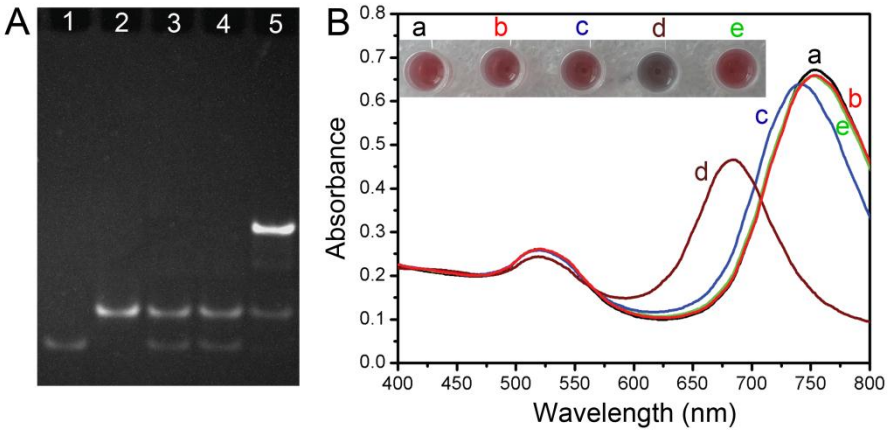

Fig. 2 (A) Non-denaturing PAGE image of CHA products: H1 (lane 1), H2 (lane 2), H1+H2 (lane 3), TS+H1+H2 (lane 4), and TEP+H1+H2 (lane 5). (B) UV-vis absorption spectra of AuNRs (a, black line), Au NRs+telomerase+TS (b, red line), Au NRs+H1+H2 (c, blue line), Au NRs+telomerase+TS+H1+H2 (d, brown line), and Au NRs+inactive telomerase+TS+H1+H2 (e, green line). Inset, typical photographs of the colloidal solutions corresponding to the UV-vis spectra. Telomerase corresponding to 1000 HeLa cells was used.

3.3 Optimization of experimental conditions

The longitudinal LSPR peak shift of Au NRs ($\Delta\lambda$) was used for evaluation of the sensing performance. Firstly, we optimized the etching conditions, including concentrations of CTAB and HCl. The concentration of CTAB plays a vital role in etching of Au NRs, because CTAB can complex with Au to lower the redox potential of [$AuBr_2^-$-CTA^+]/Au (Tsung et al., 2006). For TMB^{2+}, the redox potential is in the range of 0.22-0.70 V, which is higher than that of [AuBr2−-CTA+]/Au pair (Yu et al. 2018). Consequently, the TMB^{2+} can effectively oxidize Au NRs into $AuBr_2^-$ with the assistance of CTAB. As revealed in Fig. 3A, the $\Delta\lambda$ was slight without CTAB and increased sharply with the augment of the CTAB concentration from 0.02 to 0.08 M, and then almost reached a plateau when the concentration higher than 0.08 M. Considering that high concentration CTAB owns higher viscosity, which could influence the uniform etching of AuNRs, 0.08 M of CTAB was chosen as the optimal condition. Meanwhile, the concentration of HCl was optimized to 0.20 M (Fig. 3B). The sensing performance was also affected by the efficiency of the CHA process. To achieve the best signal-to-background ratio, the concentration of hairpins and reaction time were optimized. Obviously, the $\Delta\lambda$ reached the maximum when the concentration of hairpins was 300 nM (Fig. 3C). In addition, reaction time, which determined the cycle times, was explored (Fig. 3D)**.** The $\Delta\lambda$ exhibited a time-dependent increase and reached a saturation value after 60 min, suggesting the equilibrium state of the hybridization. Thus, the hairpin concentration of 300 nM and the reaction time of 60 min were adopted in the subsequent experiments.

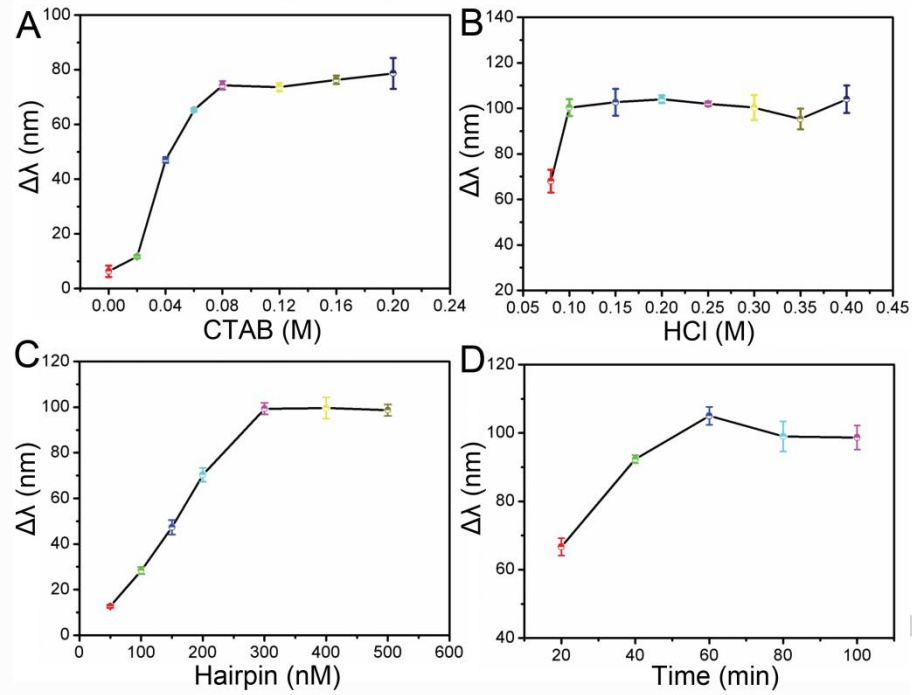

Fig. 3 Optimization of the experimental condition: the concentrations of CTAB (A) and HCl (B) during etching reaction, and the concentrations of hairpin DNA (C) and the reaction time (D) for the CHA process. The error bars represent the standard deviation of three measurements.

3.4 Detection of telomerase activity

To evaluate the analytical performance of the proposed biosensing method of telomerase activity, telomerase extracted from 1.0×10^6 HeLa cells were serially diluted in 1×CHAPS lysis buffer. A conventional TRAP assay was employed to confirm the existence and activity of telomerase in the cell extracts. As Fig. S2 shown, in the presence of active telomerase in cancer cell extract (lane 1, 2 and 3), the repeating bands of telomerase elongation products were observed at the position of 50 bp. For human normal cells (lane 4), the intensity of the band at 50 bp was relatively low and no repeating band was observed, which is because the fact that the expression of telomerase in normal cell was inhibited. Moreover, for cell extracts with the heated-inactive telomerase (lane 5) or without telomerase (lane 6), there is no band of telomerase product. Since the telomerization is controlled by the content of telomerase in the cell lysate, and more HeLa cells mean more telomerase, the signal should be correlated to the number of HeLa cells. Under the optimal conditions, the color variation and the peak shift of the longitudinal LSPR induced by telomerase in cell lysate were studied. As shown in Fig. 4A, the color changed obviously from red to brownish, gray, cyan, purple, violet and blue, as the HeLa cell number increased from 0 to 15000, which could be easily distinguished by the naked eye. As shown in Fig. 4B, the longitudinal LSPR of Au NRs blue shifted constantly from 762 to 528 nm with the increment in the number of HeLa cells, which indicates the longitudinal LSPR shift of Au NRs (Δλ) is closely related to the number of HeLa cells. Notably, the correlation of Δλ and the number of HeLa cells was plotted in Fig. 4C. And a good linear relationship was obtained in the range of 20-500 cells with a reliable correlation coefficient of 0.9890 (Fig. 4D). The detection limit was calculated according to the rule of three times standard deviation of background (3σ) divided by the slope of the standard curve, and was estimated to be as low as 15 HeLa cells. Certainly, the high sensitivity

of our assay was attributed to the signal amplification strategy of CHA. The detection limit of our assay was compared with that of other colorimetric assays for telomerase detection, as shown in Table S2.

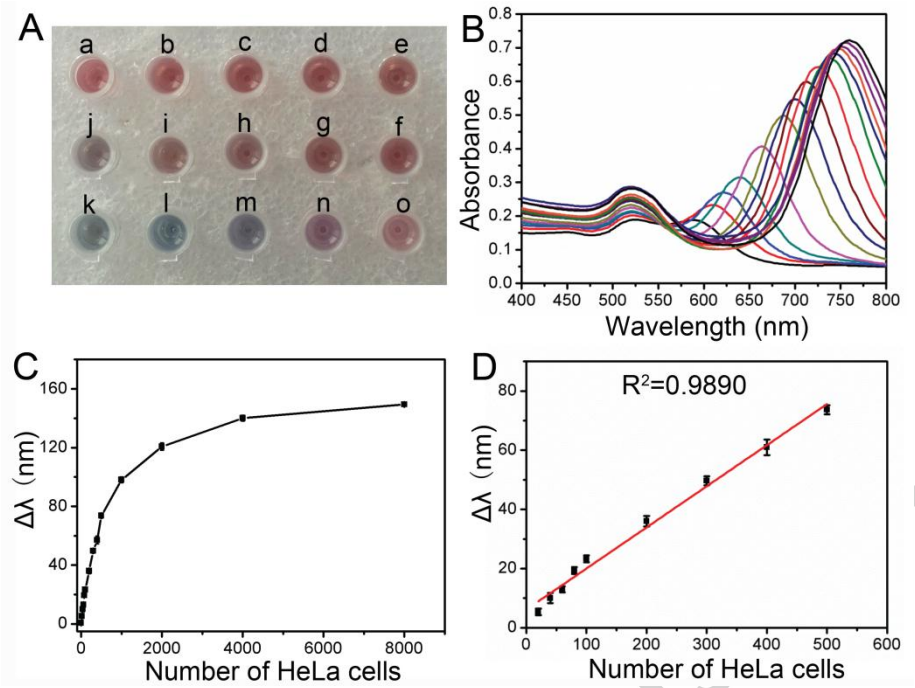

Fig. 4 Color variation (A) and corresponding UV-vis absorption spectra (B) of Au NRs in response to telomerase extracts from different number of HeLa cells in the range from 0 to 15000. From a to o, the number of HeLa cells are respectively 0, 20, 40, 60, 100, 200, 400, 600, 800, 1000, 2000, 4000, 8000 and 15000. (C) Plot of Δλ versus the number of HeLa cells in the range from 0 to 8000. (D) Linear relationship between the Δλ and HeLa cell number ranging from 0 to 500 with an equation of $y = 0.1390x + 6.1252$. The error bars represent the standard deviation of three measurements.

To further explore the morphological change of Au NRs, some typical TEM images were presented in Fig. 5. TEM images revealed that the longitudinal length of Au NRs gradually reduced with the number of HeLa cells increasing, while the transverse length remained constant, which is arising from the fact that the etching reaction preferentially occurred on the tips of Au NRs. When the telomerase level elevated to 8000 HeLa cells, the rod-like shape was lost and the spherical particles were obtained. The etching process was consistent with our expectation.

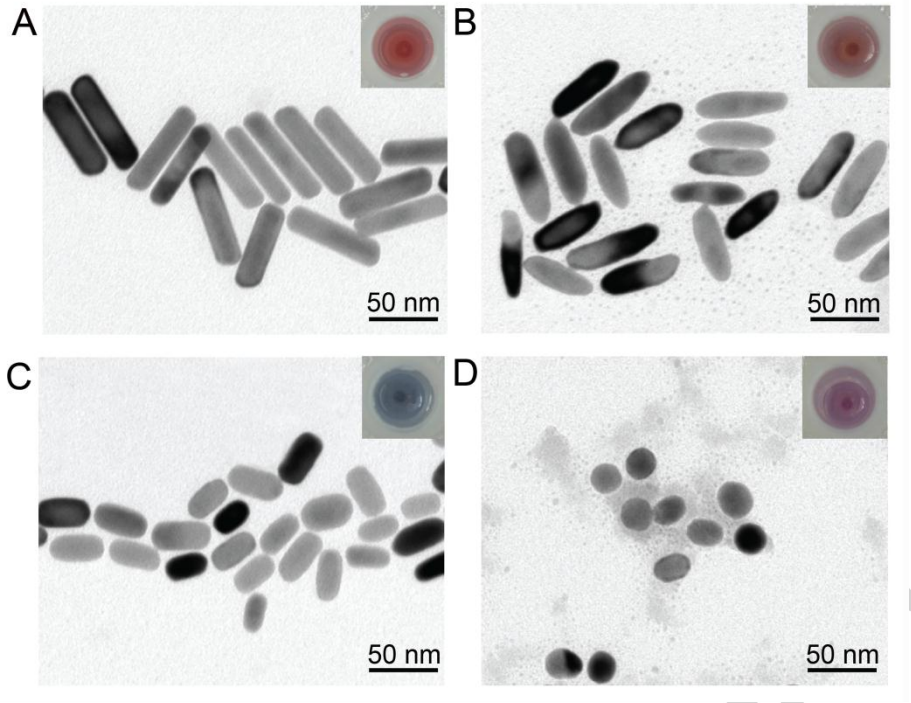

Fig. 5 The typical TEM images of Au NRs in the presence of different numbers of HeLa cells, (A) 0, (B) 100, (C) 2000 and (D) 8000. The insets of (A)-(D) show the photographs of the corresponding colloidal solutions.

4. In conclusion

In summary, by employing etching of Au NRs as a visual signal reporter and CHA as a signal amplifier, a visual and sensitive method to determine telomerase activity was successfully developed. To our knowledge, it is the first time to integrate etching-based plasmonic biosensing with CHA signal amplification strategy to detect telomerase activity. In our proposed strategy, the CHA process was specifically triggered and accumulated massive G-quadruplexes/hemin DNAzymes for the quantitative oxidation of TMB into TMB^{2+}. The TMB^{2+} could etch the Au NRs, which resulted in notable LSPR shift. The visual multiple colors were presented owing to the LSPR shift of Au NRs, and could be easily distinguished with naked eyes. Therefore, telomerase activity not only can be detected via UV-vis measurement but also can be directly observed by naked eyes. Due to the combination of the cyclic amplification strategy, the detection limit of our assay was as low as 15 HeLa cells, which is comparable to or even lower than that of other colorimetric assays. Furthermore, compared with ·OH-induced etching reaction, our approach exhibited higher stability because the introduction of HCl not only turned TMB^{+} into TMB^{2+} but also terminated DNAzyme-catalyzed oxidation reaction. This proposed strategy will make the multicolor visual detection greatly valuable in telomerase-related cancer early diagnosis and drug screening.

Acknowledgements

This work was supported by the National Natural Science Foundation of China (21874015 and 21675020) and Key Laboratory of Supramolecular Structure and Materials (Grant No. SKLSSM201824).

References

Blackburn, E.H., 1991. Nature 350 (6319), 569-573.

Cheng, W., Zhang, Y., Yu, H., Diao, W., Mo, F., Wen, B., Cheng, W., Yan, Y., 2018. Sens. Actuators B: Chem. 255, 3298-3304.

Dai, J., He, H., Duan, Z., Guo, Y., Xiao, D., 2017. Anal. Chem. 89 (22), 11971-11975.

Duan, R., Wang, B., Zhang, T., Zhang, Z., Xu, S., Chen, Z., Lou, X., Xia, F., 2014. Anal. Chem. 86 (19), 9781-9785.

Freeman, R., Sharon, E., Teller, C., Henning, A., Tzfati, Y., Willner, I., 2010. ChemBioChem 11 (17), 2362-2367.

Fu, A.C., Hu, Y., Zhao, Z.-H., Su, R., Song, Y., Zhu, D., 2018. Sens. Actuators B: Chem. 259, 642-649.

Gao, Y., Xu, J., Li, B., Jin, Y., 2016. Biosens. Bioelectron. 81, 415-422.

Kim, N.W., Piatyszek, M.A., Prowse, K.R., Harley, C.B., West, M.D., Ho, P.L.C., Coviello, G.M., Wright, W.E., Weinrich, S.L., Shay, J.W., 1994. Science 266 (23), 2011-2015.

Kong, Q., Cui, K., Zhang, L., Wang, Y., Sun, J., Ge, S., Zhang, Y., Yu, J., 2018. Anal. Chem. DOI: 10.1021/acs.analchem.8b01844

Lee, C.Y., Jang, H., Park, K.S., Park, H.G., 2017. Nanoscale 9 (42), 16149-16153.

Li, H., Fu, H.-W., Zhao, T., Kong, D.-M., 2015. RSC Adv. 5 (9), 6475-6480.

Li, J., Lei, P., Ding, S., Zhang, Y., Yang, J., Cheng, Q., Yan, Y., 2016. Biosens. Bioelectron. 77, 435-441.

Liao, H., Liu, G., Liu, Y., Li, R., Fu, W., Hu, L., 2017. Chem. Commun. 53 (73), 10160-10163.

Liu, S., Zhao, S., Tu, W., Wang, X., Wang, X., Bao, J., Wang, Y., Han, M., Dai, Z., 2017a. Chem. Eur. J. 24 (15), 3677-3682.

Liu, X., Wei, M., Xu, E., Yang, H., Wei, W., Zhang, Y., Liu, S., 2017b. Biosens. Bioelectron. 91, 347-353.

Ma, W., Fu, P., Sun, M., Xu, L., Kuang, H., Xu, C., 2017a. J. Am. Chem. Soc. 139 (34), 11752-11759.

Ma, X., Lin, Y., Guo, L., Qiu, B., Chen, G., Yang, H.-h., Lin, Z., 2017b. Biosens. Bioelectron. 87, 122-128.

Scarabelli, L., Grzelczak, M., Liz-Marzán, L.M., 2013. Chem. Mater. 25 (21), 4232-4238.

Shay, J.W., Bacchetti, S., 1997. European Journal of Cancer 33 (5), 787-791.

Shay, J.W., Wright, W.E., 2005. Carcinogenesis 26 (5), 867-874.

Shi, M., Zheng, J., Liu, C., Tan, G., Qing, Z., Yang, S., Yang, J., Tan, Y., Yang, R., 2016. Biosens. Bioelectron. 77, 673-680.

Singh, S., Mitra, K., Shukla, A., Singh, R., Gundampati, R.K., Misra, N., Maiti, P., Ray, B., 2017. Anal. Chem. 89 (1), 783-791.

Truong, P.L., Ma, X., Sim, S.J., 2014. Nanoscale 6 (4), 2307-2315.

Tsung, C.K., Kou, X., Shi, Q., Zhang, J., Yeung, M.H., Wang, J., Stucky, G.D., 2006. J. Am. Chem. Soc. 128, 5352-5353.

Wang, L.-j., Zhang, Y., Zhang, C.-y., 2013. Anal. Chem. 85 (23), 11509-11517.

Xu, Y., Zhou, W., Zhou, M., Xiang, Y., Yuan, R., Chai, Y., 2015. Biosens. Bioelectron. 64, 306-310.

Yaku, H., Yoshida, Y., Okazawa, H., Kiyono, Y., Fujita, Y., Miyoshi, D., 2017. Anal. Chem. 89 (13), 6948-6953.

Yang, K., Huo, M., Guo, Y., Yang, Y., Wu, J., Ding, L., Ju, H., 2017. Analyst 142 (19), 3740-3746.

Ye, X., Jin, L., Caglayan, H., Chen, J., Xing, G., Zheng, C., Doan-Nguyen, V., Kang, Y., Engheta, N., Kagan, C.R., Murray, C.B., 2012. ACS Nano 6 (3), 2804-2817.

Yu, X., Lin, Y., Wang, X., Xu, L., Wang, Z., Fu, F., 2018. Microchim. Acta 185 (5), 259-268.

Zhang, L., Zhang, S., Pan, W., Liang, Q., Song, X., 2016. Biosens. Bioelectron. 77, 144-148.

Highlights

- A sensitive multicolor visual method was designed to detect telomerase activity.
- Multiple colors were displayed based on target-induced etching of Au nanorods.
- Signal was remarkably amplified thanks to the facile strategy of CHA.
- A highly sensitive detection toward telomerase was realized down to 15 HeLa cells.